IMA Journal of Applied Mathematics Advance Access published June 18, 2015

IMA Journal of Applied Mathematics (2015) Page 1 of 17
doi:10.1093/imamat/hxv016

Liquid-bridge shape stability by energy bounding

J. B. Bostwick*
Department of Engineering Science and Applied Mathematics, Northwestern University, Evanston, IL 60208, USA
*Corresponding author: joshua.bostwick@northwestern.edu

AND

P. H. Steen
School of Chemical and Biomolecular Engineering and Center for Applied Mathematics, Cornell University, Ithaca, NY 14853, USA

[Received on 7 August 2014; revised on 13 April 2015; accepted on 3 June 2015]

A liquid stretched between two solid boundaries forms a liquid bridge. The static stability ('shape stability') of the liquid bridge to disturbances whose contact-line is (i) pinned or (ii) moves with fixed contact-angle is studied. The liquid/gas interface is idealized as a mathematical surface of constant surface tension. Elementary results from the calculus-of-variations are utilized to derive a sufficient condition for stability without explicitly solving the boundary value problem associated with the second variation. The focus is generating 'quick' checks on stability. The utility of the method is illustrated by limiting cases of the liquid bridge between parallel plates; the liquid cylinder and catenoid. Our stability criteria gives sharp bounds in some cases, recovering previously reported results and yields new predictions for mobile contact-line disturbances. We conclude with remarks concerning the effect of support geometry.

Keywords: interfacial stability; capillarity; variational methods.

1. Introduction

A volume of liquid that makes separate contact with two solid surfaces is referred to as a 'liquid bridge', a 'liquid bead' or sometimes, if the curved solids are convex to one another, a 'pendular ring'. To emphasize that the liquid is held in place by surface tension the term 'capillary bridge' may be used. We adopt the perspective of a liquid bridge surrounded by gas, rather than vice versa, for definiteness, although the equilibrium shape and stability of a gas bridge surrounded by liquid are the same, provided body forces such as gravity are negligible. The overall shape of the bridge is given by its entire boundary, the union of the liquid/gas and the liquid/solid interfaces. However, for non-deformable solids, the liquid/solid interface remains a fixed shape and any liquid/solid influence on the liquid/gas shape occurs at the three-phase common line, or 'contact line.' Hence, shape instability refers to the shape changes of the liquid/gas interface (or a liquid/liquid interface in the case of immiscible liquids) with a possible displacement of the contact line. In summary, we are concerned with the stability of liquid bridges, a classical subject but with a re-emerging relevance. We obtain energy stability bounds which yield sufficient conditions for stability. The simplicity of the bounding technique gives flexibility—it can be used to obtain quick estimates of stability windows or to perform checks on 'exact' windows from more computationally intensive solutions.

Capillary bridges are found in nature and in industry. For typical liquids, the capillary length scale varies from many centimetres in a low gravity environment, as on board the International Space Station, to a few millimetres in earth bound applications. Bridge shape instability has been widely studied as relevant to space applications (Bauer, 1992; Langbein, 2002), enhanced oil recovery (Olbricht, 1996), reversible capillary adhesion (Vogel & Steen, 2010), sintering of matter into porous structures (Carter, 1988), drug delivery (Elele *et al.*, 2010) and gravure printing (Dodds *et al.*, 2012).

Equilibria are shapes of constant mean curvature. That is, starting from an energy functional which takes into account liquid/gas interfacial energy, one obtains the Euler–Lagrange equation for the stationary states, which is recognized as the Young–Laplace equation. For axisymmetric bridges, the constant curvature states have been fully characterized by Delaunay (1841). They consist of unduloids and nodoids, with the catenoids and spheres as limiting cases (Gillette & Dyson, 1971).

The static stability of any equilibrium shape is simple to determine, in principle. Disturb the shape and calculate the energy rise or fall relative to the base state. A base state for which all non-trivial disturbances give higher energies is 'stable'. If one disturbance gives a lower energy, the state is 'unstable' whereas, if neither stable nor unstable, the state is called 'neutral.'

The static formulation does not encompass growth rates associated with the hydrodynamic problem. However, static stability bounds are known to carry forward to the hydrodynamic description (Davis, 1980; Bostwick & Steen, 2013). Stability determination can be subtle, in practice however. This is because stability depends sensitively on the class of disturbances against which the base state is tested, as outlined in the recent review by Bostwick & Steen (2015). For example, the same equilibrium state may be stable against volume-preserving disturbances but unstable against constant pressure disturbances. Or the same equilibrium state may be stable against fixed contact-line disturbances but unstable if the disturbed contact-line is allowed to move. When two or three-parameter families of disturbances are considered, the determination can become complicated. Gillette & Dyson (1974) noted that, in the case of determining the stability of the catenoid under constraint, even Maxwell (1898) got it wrong.

Bridge stability is sensitive to contact-line boundary conditions. We consider disturbances whose contact-line is (i) pinned or (ii) moves with fixed contact-angle α, which is defined by the Young–Dupré equation (Young, 1805; Dupré, 1869),

$$\sigma_{\rm sg} - \sigma_{\rm ls} = \sigma \cos\alpha. \tag{1.1}$$

Here the liquid/gas σ, liquid/solid $\sigma_{\rm ls}$ and solid/gas $\sigma_{\rm sg}$ interfacial tensions define the wetting properties of the solid substrate through the static contact-angle α. One must also distinguish between disturbances that (i) do or (ii) do not preserve the volume enclosed by the equilibrium surface. That is, for each contact-line condition, we treat the constant volume and constant pressure disturbance as separate subcases. We then classify the disturbances in terms of relative stability showing that pressure disturbances with moving contact-lines are the most dangerous (most destabilizing), while volume disturbances with pinned contact-lines are the least dangerous (least destabilizing).

A number of approaches can be used to determine stability. A classical approach, rooted in the work of Weierstrass, addresses directly the second variation of the energy functional. To prove stability one must show the second variation is positive by (i) satisfying Legendre's condition and (ii) proving the absence of a conjugate point or negative eigenvalue of Jacobi's equation (Bolsa, 1904; Young, 2000). With regard to capillary surfaces, the stability calculation may be complicated further by a volume conservation constraint, a necessary condition for incompressible fluids. Howe (1887) uses the conjugate point criteria to generate stability results for the zero-gravity, axisymmetric capillary surface

(Gillette & Dyson, 1971). Alternative solution methods rely on the observation that stability limits occur at turning points of a preferred bifurcation diagram (Poincaré, 1885; Padday & Pitt, 1973; Vogel, 1989). Maddocks (1987) states and proves the relevant theorems on constrained variational principles and embedding of bifurcation parameters, while the review by Michael (1981) illustrates the many ways that bifurcation theory applies to meniscus stability. Lowry & Steen (1995) apply the aforementioned Poincaré–Maddocks theorems to study the stability of the general liquid bridge with pinned contact lines using continuation techniques. The method works well in circumstances where the critical disturbance is axisymmetric (Gillette & Dyson, 1972), but breaks down when the critical disturbance is non-axisymmetric (Russo & Steen, 1986).

In contrast to direct calculation, we work indirectly with the second variation using elementary results from the calculus-of-variations to derive static stability bounds for the family of liquid bridges. The goal is to produce quick stability results (checks) for the practitioner. Our analysis parallels that of Davis (1980), who considered the stability of the static rivulet under a number of contact-line conditions. Our approach relies upon bounding a quadratic form related to the second variation. It gives sufficient conditions for stability. These represent bounds on the second-order energy difference. We illustrate the utility of our method by comparing our results for the liquid cylinder to the classic Plateau limit and to those reported by Erle *et al.* (1970) for the symmetric catenoid with pinned contact-lines, both of which are limiting cases of the liquid bridge. In addition, we report stability limits for the catenoid with a mobile contact-line at one or both solid supports. These results are new, as far as we are aware. Finally, we also compare with the exact stability window for the symmetric fixed contact-line bridge, a well-studied case, and extend our analysis to the cases for one or two mobile contact-lines.

We begin this paper by defining the second variation of surface energy for the liquid bridge and the relevant boundary conditions on the solid supports, which define the interface disturbance. The second variation is then manipulated into a quadratic form, which we bound to generate a critical functional from which we derive our stability criteria. We compare our bounding method with the classic stability limits for the liquid cylinder and symmetric catenoid. Our bounding result is sharp in these cases. Next, we extend our analysis to report new stability results for the asymmetric catenoid and most-general symmetric liquid bridge between parallel plates with mobile contact-lines. We conclude with some remarks on the relevance of our method.

2. Liquid bridge

A capillary surface $\boldsymbol{x} = \boldsymbol{r}(u, v)$ with intrinsic surface coordinates u, v has an energy U proportional to its surface area

$$U/\sigma = A = \int |\boldsymbol{r}_u \times \boldsymbol{r}_v| \, \mathrm{d}u \, \mathrm{d}v, \tag{2.1}$$

with σ the liquid/gas surface tension. Equilibrium surfaces are extremals of the energy functional that satisfy the first-order condition $\delta U = 0$. For capillary surfaces, the resulting Euler–Lagrange equation for the energy functional (2.1) is more commonly referred to as the Young–Laplace equation (Young, 1805; Laplace, 1806),

$$p/\sigma = \kappa_1 + \kappa_2 \equiv 2H, \tag{2.2}$$

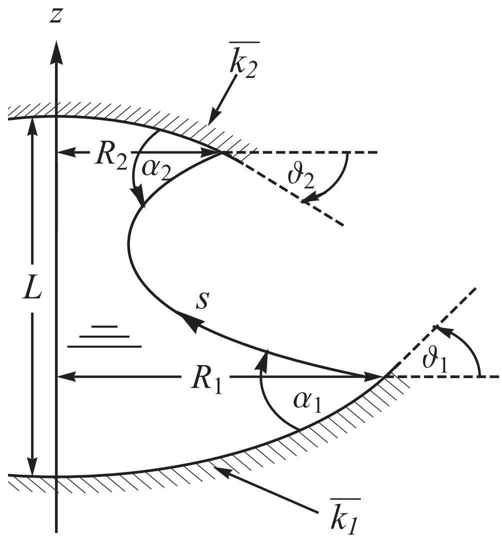

FIG. 1. Definition sketch of the liquid bridge in axisymmetric coordinates (r, z) with axial length L spanned between solid supports with bounding radii R_1, R_2 and contact-angles α_1, α_2. The upper and lower support surfaces have normal curvatures $\bar{k}_2$ and $\bar{k}_1$ and filling angles ϑ_2 and ϑ_1, respectively.

which relates the principal curvatures κ_1, κ_2 (equivalently, the mean curvature H) to the pressure p. The liquid bridge is an equilibrium surface that can be described parametrically using pseudo-arclength $s \in [-1/2, 1/2]$ and azimuthal angle $\varphi \in [0, 2\pi]$ as surface coordinates. For axisymmetric shapes, the functions (r, z) satisfy the following Young–Laplace equations:

$$r''(s) = -z'(s)\left(p - \frac{z'(s)}{r(s)}\right), \quad z''(s) = r'(s)\left(p - \frac{z'(s)}{r(s)}\right),$$
$$r(-1/2) = R_1, \quad r(1/2) = R_2, \quad z(-1/2) = 0, \quad z(1/2) = L, \tag{2.3}$$

where $' = d/ds$ denotes differentiation with respect to pseudo-arclength (Myshkis *et al.*, 1987). Here lengths have been scaled with respect to the total arclength $\mathscr{S} = 1$ so that the liquid bridge is described by its axial length L, bounding radii R_1, R_2, filling angles ϑ_1, ϑ_2 and static contact-angles α_1, α_2,

$$\cot(\alpha_1 - \vartheta_1) \equiv -\left.\frac{\mathrm{d}r/\mathrm{d}s}{\mathrm{d}z/\mathrm{d}s}\right|_{s=-1/2}, \quad \cot(\alpha_2 - \vartheta_2) \equiv \left.\frac{\mathrm{d}r/\mathrm{d}s}{\mathrm{d}z/\mathrm{d}s}\right|_{s=1/2}, \tag{2.4}$$

as shown in Fig. 1. Note that the equilibrium shape $\{r(s), z(s)\}$ can be idealized as having either a (i) fixed base radius R_1, R_2 or (ii) fixed contact-angle α_1, α_2 at each solid support (Michael & Williams, 1997). With regard to the calculus-of-variations, the latter are the ‘natural’ boundary conditions for the energy functional (2.1). Orr *et al.* (1975) solve (2.3) and (2.4) to obtain pendular ring shapes parameterized by the mean curvature, filling angles and stand-off length L. These closed form equilibrium solutions are pieces of Delaunay surfaces, of course. Their stability is not considered.

2.1 *Second variation of surface energy*

As the liquid bridge is an equilibrium surface, stability is determined by solving the eigenvalue problem associated with the second variation (c.f. Blaschke, 1930, section 116, Myshkis *et al.*, 1987).

$$-\Delta_\Gamma \eta(s,\varphi) - (\kappa_1^2+\kappa_2^2)\eta(s,\varphi) = \lambda\eta(s,\varphi), \tag{2.5}$$

where $\eta(s,\varphi)$ is the linearized surface disturbance. The sign of the eigenvalue λ gives the stability result; $\lambda > 0$ implies the equilibrium surface is a stable configuration, whereas $\lambda < 0$ corresponds to an unstable configuration. Here the Laplace–Beltrami operator,

$$\Delta_\Gamma \eta = \frac{1}{\sqrt{g}}\frac{\partial}{\partial u^\alpha}\left(\sqrt{g}g^{\alpha\beta}\frac{\partial\eta}{\partial u^\beta}\right), \tag{2.6}$$

is defined on the equilibrium surface through the surface metric

$$g_{\alpha\beta} = [g^{\alpha\beta}]^{-1} \equiv \boldsymbol{x}_\alpha \cdot \boldsymbol{x}_\beta = \begin{pmatrix} r'^2+z'^2 & 0 \\ 0 & r^2 \end{pmatrix}, \quad g = r^2(r'^2+z'^2). \tag{2.7}$$

2.1.1 *Derivation of the stability criteria* Rather than explicitly constructing a solution to the boundary value problem (2.5), we choose to work directly with the second variation. We begin by assuming, from periodicity, that the surface disturbance can be expanded as

$$\eta(s,\varphi) = y(s)\mathrm{e}^{i\ell\varphi}, \quad \ell = 0,1,2,\ldots, \tag{2.8}$$

where ℓ is the polar wavenumber. Applying the surface metric (2.7) and the ansatz (2.8) to the integral form of the second variation (2.5) results in the following functional equation

$$\int_{-1/2}^{1/2} (-y''y - F(s)y'y - G(s;\ell)y^2)\,\mathrm{d}s = \lambda\int_{-1/2}^{1/2} g_{ss}y^2\,\mathrm{d}s, \tag{2.9}$$

where

$$F(s) \equiv \frac{(\sqrt{g_{\varphi\varphi}/g_{ss}})'}{\sqrt{g_{\varphi\varphi}/g_{ss}}},\ G(s;\ell) \equiv g_{ss}\left(\kappa_1^2+\kappa_2^2-\frac{\ell^2}{g_{\varphi\varphi}}\right). \tag{2.10}$$

This is sometimes referred to as the disturbance energy. It is straightforward to show that the right-hand side of (2.9) is positive definite. Hence, stability is uniquely determined by the sign of the functional

$$I(\ell) \equiv -\int_{-1/2}^{1/2} (y'' + F(s)y' + G(s;\ell)y)y\,\mathrm{d}s. \tag{2.11}$$

We formulate a stability criteria by first integrating I by parts to yield

$$\int_{-1/2}^{1/2}\left(y'^2 - \left(G(s;\ell)-\frac{1}{2}F'(s)\right)y^2\right)\mathrm{d}s - yy'|_{-1/2}^{1/2} - \frac{F(s)}{2}y^2\bigg|_{-1/2}^{1/2} \tag{2.12}$$

which is a quadratic form that can be bounded using the extreme value theorem (Stewart, 1995). A lower bound on the functional I is given by

$$I_{\min} \equiv \int_{-1/2}^{1/2} (y'^2 - My^2)\,\mathrm{d}s - yy'|_{-1/2}^{1/2} - \frac{F(s)}{2} y^2 \bigg|_{-1/2}^{1/2}, \tag{2.13}$$

where the scalar M is defined as

$$M(\ell) \equiv \max_{s\in[-1/2,1/2]} \left(G(s;\ell) - \frac{1}{2}F'(s) \right). \tag{2.14}$$

It follows that the liquid bridge is stable to allowable disturbances when $I_{\min} > 0$. The functional $I_{\min}$ is dependent upon the boundary conditions at the contact-lines, which we analyse separately.

2.2 *Contact-line boundary conditions*

The second variation of interfacial energy (2.5) is augmented with boundary conditions at the contact-lines $s = \pm 1/2$. We implement three different contact-line conditions that are all consistent with the variation of the boundary conditions associated with either a (i) fixed base radius or (ii) fixed contact-angle at each solid support. The first disturbance (pin–pin) has pinned contact-lines at both solid supports,

$$y(-1/2) = y(1/2) = 0, \tag{2.15}$$

while the second disturbance (pin-free) has a pinned contact-line at the lower support ($s = -1/2$) and a mobile contact-line that preserves the static contact-angle α_2 at the upper support ($s = 1/2$),

$$y(-1/2) = 0, \quad y'(1/2) + (k(1/2)\cot\alpha_2 - \bar{k}_2/\sin\alpha_2)y(1/2) = 0. \tag{2.16}$$

Here $k(s)$ is the normal curvature of the equilibrium surface. The third disturbance (free-free) has mobile contact lines at both the upper and lower supports,

$$\begin{aligned} -y'(-1/2) + (k(-1/2)\cot\alpha_1 - \bar{k}_1/\sin\alpha_1)y(-1/2) &= 0, \\ y'(1/2) + (k(1/2)\cot\alpha_2 - \bar{k}_2/\sin\alpha_2)y(1/2) &= 0. \end{aligned} \tag{2.17}$$

2.3 *Volume conservation constraint*

Lastly, we consider two types of stability that are distinguished by assumptions about our underlying fluid and/or experimental conditions. In cases where the total volume enclosed by the disturbed surface is held fixed, as with incompressible fluids, the function y must also satisfy the following condition for $\ell = 0$,

$$\int_{-1/2}^{1/2} y(s)\,\mathrm{d}s = 0. \tag{2.18}$$

We refer to disturbances that preserve volume as constrained. In contrast, disturbances that do not conserve volume are referred to as unconstrained. Alternatively, constrained and unconstrained can be referred to as constant volume and constant pressure disturbances, which hereafter we will call ‘volume disturbances’ and ‘pressure disturbances’, respectively.

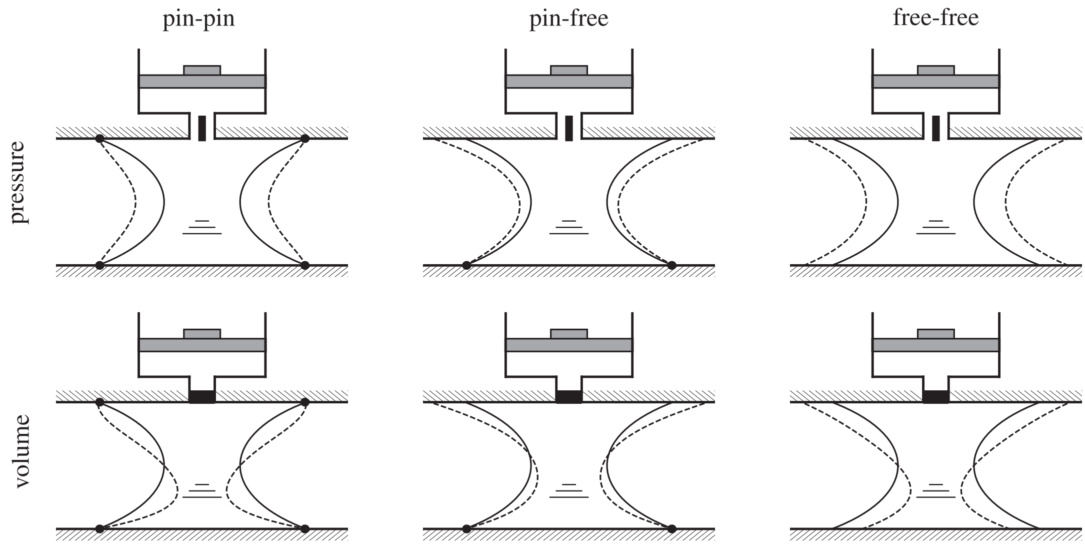

FIG. 2. Schematic of pressure (top row) and volume (bottom row) disturbances for pin–pin (left column), pin–free (centre column) and free–free (right column) boundaries on planar supports.

2.4 *Stability criteria*

We now derive a stability criteria for the specific disturbances shown in Fig. 2.

2.4.1 *Pin–Pin* We begin by applying the pinned contact-line conditions (2.15) to (2.13) to yield

$$I_{\mathrm{pp}} = \int_{-1/2}^{1/2} (y'^2 - My^2)\,\mathrm{d}s. \tag{2.19}$$

Next, we recall the following standard result from the calculus of variations, also known as the Poincaré inequality (Joseph, 1976),

$$\int_{-1/2}^{1/2} y'^2\,\mathrm{d}s \geqslant \xi^2 \int_{-1/2}^{1/2} y^2\,\mathrm{d}s. \tag{2.20}$$

which we apply to (2.19) to give

$$I_{\mathrm{pp}} \geqslant (\xi^2 - M) \int_{-1/2}^{1/2} y^2\,\mathrm{d}s. \tag{2.21}$$

Hence, the liquid bridge is stable to disturbances with pinned contact-lines if

$$\xi^2 > M. \tag{2.22}$$

Here the positive number ξ^2 is the smallest eigenvalue calculated from the associated boundary value problem

$$y'' + \xi^2 y = \mu, \quad y(-1/2) = y(1/2) = 0, \tag{2.23}$$

where μ is a Lagrange multiplier used to enforce volume conservation (2.18) for the constrained problem. For the unconstrained problem, we set $\mu = 0$ and show the smallest eigenvalue of (2.23) is $\xi = \pi$, which yields the unconstrained stability criteria

$$\pi^2 > M. \tag{2.24}$$

For the constrained problem, we augment (2.23) with the volume conservation constraint (2.18) and show the eigenvalues satisfy the characteristic equation $(\xi \sin\xi + 2\cos\xi - 2)/\xi^2 = 0$. The smallest eigenvalue $\xi = 2\pi$ generates the constrained stability criteria

$$(2\pi)^2 > M. \tag{2.25}$$

Equations (2.24) and (2.25) provide quick checks on stability for all liquid bridges with pinned contact-lines.

2.4.2 *Pin–Free* Applying the mixed boundary conditions (2.16) to (2.13) yields the reduced functional

$$I_{\mathrm{pf}} = \int_{-1/2}^{1/2} (y'^2 - My^2)\,\mathrm{d}s + A_{\mathrm{f}} y^2(1/2), \tag{2.26}$$

where

$$A_{\mathrm{f}} \equiv (k(1/2)\cot\alpha_2 - \bar{k}_2 \sin\alpha_2) - \tfrac{1}{2}F(1/2). \tag{2.27}$$

We utilize the following inequality,

$$\int_{-1/2}^{1/2} y'^2\,\mathrm{d}s + A_{\mathrm{f}} y^2(1/2) \geqslant \zeta \int_{-1/2}^{1/2} y^2\,\mathrm{d}s, \tag{2.28}$$

which is obtained from a calculus-of-variations problem whose Euler–Lagrange equations are given by

$$y'' + \zeta y = \mu, \quad y(-1/2) = 0, \quad y'(1/2) + A_{\mathrm{f}} y(1/2) = 0. \tag{2.29}$$

As before, μ is a Lagrange multiplier used to enforce volume conservation (2.18) for the constrained problem. We compute the smallest eigenvalue ζ of (2.29) for the unconstrained and constrained cases

$$I_{\mathrm{pf}} \geqslant (\zeta - M) \int_{-1/2}^{1/2} y^2\,\mathrm{d}s. \tag{2.30}$$

Stability is guaranteed provided that ζ satisfies

$$\zeta - M > 0. \tag{2.31}$$

Note that (2.29) is a standard boundary value problem.

2.4.3 *Free–Free* Finally, we apply the mobile boundary conditions (2.17) to (2.13) to arrive at the reduced functional

$$I_{\mathrm{ff}} = \int_{-1/2}^{1/2} (y'^2 - My^2)\,\mathrm{d}s + A_{\mathrm{f}} y^2(1/2) + B_{\mathrm{f}} y^2(-1/2), \tag{2.32}$$

where A_{f} is defined in (2.27) and

$$B_{\mathrm{f}} \equiv (k(-1/2)\cot\alpha_1 - \bar{k}_1 \sin\alpha_1) + \tfrac{1}{2}F(-1/2). \tag{2.33}$$

We employ the following inequality,

$$\int_{-1/2}^{1/2} y'^2\,\mathrm{d}s + A_{\mathrm{f}} y^2(1/2) + B_{\mathrm{f}} y^2(-1/2) \geqslant \chi \int_{-1/2}^{1/2} y^2\,\mathrm{d}s, \tag{2.34}$$

derived from a calculus-of-variations problem with Euler–Lagrange equations given by

$$y'' + \chi y = \mu, \quad -y'(-1/2) + B_{\mathrm{f}} y(-1/2) = 0, \quad y'(1/2) + A_{\mathrm{f}} y(1/2) = 0. \tag{2.35}$$

Here μ is a Lagrange multiplier used to enforce volume conservation (2.18) for the constrained problem and χ is the smallest eigenvalue of the boundary value problem (2.35). Equation (2.34) is applied to (2.26) to give

$$I_{\mathrm{ff}} \geqslant (\chi - M) \int_{-1/2}^{1/2} y^2\,\mathrm{d}s, \tag{2.36}$$

which implies that stability is assured provided

$$\chi - M > 0. \tag{2.37}$$

Critical disturbance The respective stability criteria are examined for the critical disturbance. Sometimes the character of the critical disturbance can be predicted *a priori*. For example, for volume disturbances with pin-pin end conditions, axisymmetric $\ell = 0$ disturbances are most dangerous to base states that are single valued in radial coordinate (Steiner, 1882; Gillette & Dyson, 1972; Bostwick & Steen, 2010). Shapes with tangents to the endplates are the limiting shapes beyond which non-axisymmetric disturbances are destabilizing (Russo & Steen, 1986; Slobozhanin *et al.*, 1997). We call this the 'Steiner limit' (SL). Elfring & Lauga (2012) have recently demonstrated that a squeezed droplet (liquid bridge) with a mobile contact-line undergoes an asymmetric buckling instability at the SL, suggesting the relevance of the limit to end conditions other than pin–pin. For liquid bridges between parallel plates (below the SL, by necessity), the critical volume disturbance for free–free conditions is axisymmetric $\ell = 0$ (Vogel, 1987, 1989; Langbein, 1992), as summarized in Langbein (2002, Section 6.1). In this paper, we report results for liquid bridges that respect the Steiner limit.

An immediate consequence of our analysis is that axisymmetric $\ell = 0$ shapes are the most dangerous pressure disturbances, irrespective of end conditions. This can be seen by examining the critical scalar M in (2.14), which is a strictly decreasing function of azimuthal wavenumber ℓ. The assumption about the axisymmetric character of the critical disturbance is not valid for all capillary systems however. For example, for a beaded drop on a fibre (internal solid support), the system energy can be lowered by shifting to the perimeter of the wire, thereby breaking axisymmetry and becoming more like an isolated drop (Quéré, 1999; Langbein, 2002). Such a configuration cannot occur between parallel supports. Moreover, instability predictions are outside the scope of this paper since our method reports

TABLE 1 *Stability limits for the liquid cylinder to pressure and volume disturbances, as defined through the aspect ratio* $1/R$ *for the pin–pin, pin–free and free–free boundary conditions*

	Pressure	Volume
Pin–pin	π	2π
Pin–free	$\pi/2$	4.49341
Free–free	0	π

stable states. For volume disturbances with pin–free or free–free end conditions, no statement can be made *a priori* and one must consider both axisymmetric $\ell = 0$ and azimuthal $\ell \neq 0$ disturbances.

3. Results

For brevity, we focus our presentation on interfaces with planar surfaces-of-support $\bar{k}_1 = \bar{k}_2 = 0$, although it would be straightforward to analyse the more general case of pendular rings (see Section 3.4).

3.1 *Cylinder*

We begin by computing the static stability limit for the Plateau instability of the liquid cylinder to compare our bounding technique with this classic result (Plateau, 1863; Rayleigh, 1879). The cylindrical interface is described parametrically as

$$r = R, \quad z = s, \quad g_{ss} = 1, \quad g_{\varphi\varphi} = R^2. \tag{3.1}$$

Here lengths are scaled with the axial length $L = 1$ so that the family of cylinders are uniquely described by their radius R (alternatively, aspect ratio or 'slenderness' $1/R$). The cylinder interface has normal curvature $k = 1/R$, principal curvatures $\kappa_1 = 1/R, \kappa_2 = 0$ and contact-angles $\alpha_1 = \alpha_2 = \pi/2$. One then uses the equilibrium surface properties to show that $F(s) = 0, G(s) = (1 - \ell^2)/R^2, M = (1 - \ell^2)/R^2$ and $A_{\mathrm{f}} = B_{\mathrm{f}} = 0$. As could be expected, since M (2.14) is constant on the entire domain, our bounding method yields the exact stability limit summarized in Table 1 (e.g. Johns & Narayanan, 2002). Note that $M(1) = 0$ and $M(\ell \geqslant 2) < 0$, demonstrating that azimuthal disturbances are always stable, as could be expected.

3.2 *Catenoid*

Next, we extend our analysis by computing the stability limits for the catenoid, which is a limiting case of the liquid bridge. The catenoid surface can be defined parametrically,

$$r = c \cosh\left(\frac{s}{c} - \beta\right), \quad z = s, \tag{3.2}$$

using pseudo-arclength $s \in [-1/2, 1/2]$ and azimuthal angle $\varphi \in [0, 2\pi]$ as generalized surface coordinates. The catenoid has principal curvatures

$$\kappa_1 = -\kappa_2 = \frac{1}{c}\,\mathrm{sech}^2\left(\frac{s}{c} - \beta\right) \tag{3.3}$$

and is distinguished by its mean curvature $2H = \kappa_1 + \kappa_2 = 0$. A surface with zero mean curvature is known as a minimal surface. The catenoid is a two-parameter (c, β) family of solutions, which can also be represented by the slenderness of the contact radii R_1, R_2,

$$\Lambda_1 \equiv \frac{L}{2R_1} = \frac{1}{2c\cosh(-1/2c - \beta)}, \quad \Lambda_2 \equiv \frac{L}{2R_2} = \frac{1}{2c\cosh(1/2c - \beta)}, \tag{3.4}$$

or, alternatively, the contact-angles α_1, α_2; $\cot\alpha_1 \equiv -\sinh(-1/2c - \beta)$, $\cot\alpha_2 \equiv \sinh(1/2c - \beta)$.

We compute the stability bounds for the catenoid by using the stability criteria derived for the general liquid bridge (2.5–2.7). The surface metric for the catenoid is given by

$$g_{\alpha\beta} = \begin{pmatrix} \cosh^2(s/c - \beta) & 0 \\ 0 & c^2\cosh^2(s/c - \beta) \end{pmatrix}, \quad g = c^2\cosh^4(s/c - \beta). \tag{3.5}$$

We apply the surface metric $g_{\alpha\beta}$ for the catenoid (3.5) to (2.10) to give

$$F(s) = 0, \quad G(s; \ell) = \frac{2}{c^2}\operatorname{sech}^2\left(\frac{s}{c} - \beta\right) - \frac{\ell^2}{c^2}, \tag{3.6}$$

$$A_{\mathrm{f}}(c, \beta) \equiv \frac{1}{c}\operatorname{sech}\left(\frac{1}{2c} - \beta\right)\tanh\left(\frac{1}{2c} - \beta\right), \quad B_{\mathrm{f}}(c, \beta) \equiv -\frac{1}{c}\operatorname{sech}\left(-\frac{1}{2c} - \beta\right)\tanh\left(-\frac{1}{2c} - \beta\right), \tag{3.7}$$

and

$$M = M_c(c, \beta; \ell) \equiv \max_{s \in [-\frac{1}{2}, \frac{1}{2}]}\left(\frac{2}{c^2}\operatorname{sech}^2\left(\frac{s}{c} - \beta\right) - \frac{\ell^2}{c^2}\right). \tag{3.8}$$

The stability criteria for the pin–pin (2.24, 2.25), pin–free (2.31), and free–free (2.37) disturbances are readily computed. Figure 3 shows the associated stability diagrams for $\ell = 0$. Recall that these are the most dangerous disturbances.

3.2.1 *Prior results compared: symmetric catenoid* The mirror-symmetric catenoid $\beta = 0$ has bounding radii $R_1 = R_2 \equiv R$, contact-angles $\alpha_1 = \alpha_2 \equiv \alpha$ and critical parameter $M_c(c, 0; 0) = 2/c^2$. Given the critical parameter M_c, the stability limit for the pin–pin disturbance follows immediately from (2.24, 2.25); $c = \sqrt{2}/\pi$ for unconstrained and $1/\sqrt{2}\pi$ for constrained stability, respectively. Erle *et al.* (1970) report stability limits for the same problem in terms of the slenderness; $\Lambda_u^E = 0.662$ and $\Lambda_c^E = 0.472$ for unconstrained and constrained stability, respectively. Our stability bounds are reported in Table 2, $\Lambda_u = 0.660$ and $\Lambda_c = 0.476$. Note that our stability results differs from Erle *et al.* (1970) only at the third decimal. Hence, we have shown that our bounding method produces sharp results in this case, as witnessed by the 0.01% error in the critical slenderness. Table 2 summarizes the stability limits for the symmetric catenoid using both the parameter c and the slenderness $\Lambda \equiv L/2R$.

3.2.2 *Remarks* As we have shown, our method is sharp, being able to reproduce the well-known stability limits for the symmetric catenoid subject to pin–pin disturbances (Erle *et al.*, 1970). We also report stability limits to disturbances with mobile contact-lines at one (pin–free) or both (free–free) solid supports. As indicated, *we are unable* to find a bound for the symmetric catenoid with mobile contact-lines (free–free) that gives a sufficient condition for stability. This result is perhaps not surprising, considering

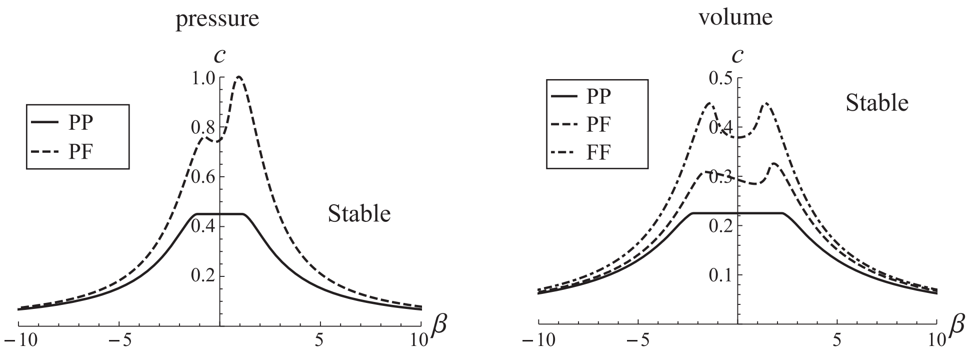

FIG. 3. Catenoid stability diagram for $\ell = 0$ in the (c, β) parameter space for pin–pin (PP), pin–free (PF) and free–free (FF) contact-lines shows nested stability windows for pressure and volume disturbances. Note the different vertical scales in the subfigures.

TABLE 2 *Stability limits for the symmetric catenoid $\beta = 0$ to pressure and volume disturbances with $\ell = 0$, as measured by the critical parameter c^* and slenderness Λ^* for the pin–pin, pin–free and free–free conditions*

	Pressure (c^*, Λ^*)	Volume (c^*, Λ^*)
Pin–pin	(0.450158, 0.659991)	(0.225078, 0.476238)
Pin–free	(0.746505, 0.543297)	(0.293174, 0.599919)
Free–free	$(\infty, 0)$	(0.378667, 0.658232)

that as the contact-line moves along the surface-of-support, volume is constantly allowed to leave the domain, resulting in the collapse of the catenoid upon itself. There is no physical mechanism to resist collapse. For the constrained case, our computation reveals stability for $c > c^* = 0.37886$, which coincides with a contact-angle $\alpha > \alpha^* = 29.91°$. Here the volume conservation condition is relatively stabilizing and acts like a restoring force to the contact-line motion. More generally, Table 2 shows that volume disturbances are less dangerous than pressure disturbances for every contact-line condition we consider here.

With regard to the contact-line boundary conditions, according to our bounds, Table 2 shows the pin–pin disturbance is relatively stable to the pin–free disturbance and the pin–free disturbance is relatively stable to the free–free disturbance. Figure 3 shows the associated nesting of stability windows. This implies that a capillary surface that is stable to free–free disturbances is also stable to pin–free and pin–pin disturbances. When viewed in the variational sense, constraints tend to stabilize by restricting the class of allowable solutions, as is the case with the pinned contact-line. The same reasoning applies to the volume (constrained) and pressure (unconstrained) disturbances. To summarize, the unconstrained (pressure) free–free disturbance is the most dangerous or least stabilizing, while the constrained (volume) pin–pin contact-line is the most stabilizing. This stands as a principle (Bostwick & Steen, 2015).

3.3 *General liquid bridge*

We have shown that the bounding method is sharp for the well-known stability limits for the liquid cylinder and symmetric catenoid with pinned contact lines. In addition, we have extended our analysis

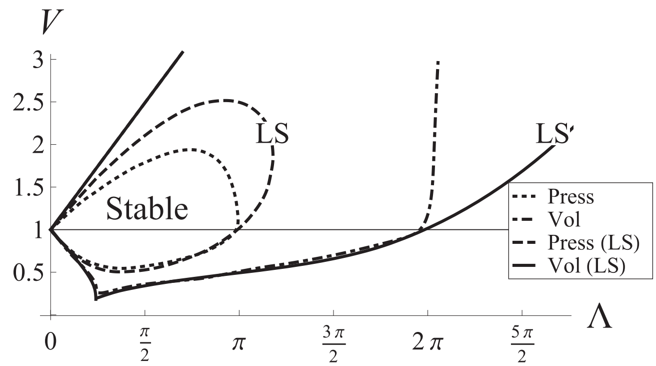

FIG. 4. Symmetric liquid bridge stability diagram in the length–volume (Λ, V) space for pin–pin conditions to compare the bounding technique with computations by Lowry & Steen (1995) (LS) for pressure and volume disturbances.

by computing the stability bounds for the more general asymmetric catenoid with mobile contact lines. These results are new, as far as we are aware.

Next, we consider the most general liquid bridge of length L and equal bounding radii $R_1 = R_2 = R$ to further explore the limits of applicability for the bounding method. We represent the liquid bridge in the length–volume (Λ, V) space,

$$\Lambda \equiv \frac{L}{2R}, \quad V \equiv \frac{\int_{-1/2}^{1/2} r^2(s) z'(s)\, \mathrm{d}s}{R^2 L}, \tag{3.9}$$

so as to directly compare with exact results for pin–pin disturbances (Gillette & Dyson, 1971; Lowry & Steen, 1995; Slobozhanin *et al.*, 1997). Here the bridge length is scaled by the bounding radius R and volume with that of a cylinder $V_{cyl} = \pi R^2 L$.

Figure 4 plots the stability diagram in the length–volume (Λ, V) space for the axisymmetric liquid bridge with pin–pin boundary conditions to compare the 'exact' results with those predicted by the bounding method. As shown, the bounding method is sharp for slender bridges $V < 1$, reproducing the 'exact' stability bounds reported by Lowry & Steen (1995). For fat bridges $V > 1$, we are able to predict a large portion of the full stable states, but not all of them. In general, one could say that the bounding method works well for slender bridges. This suggests that the newly reported stability bounds for the asymmetric catenoid with mobile contact-lines is sharp, as the catenoid is a slender liquid bridge. Lastly, we report the stability bounds for the symmetric liquid bridge for the pin–free (Fig. 5(a)) and free–free (Fig. 5(b)) boundary conditions. Note that we are unable to find any region of stability to constant–pressure disturbances with free–free boundary conditions. These results are new, as far as we are aware.

3.4 *Support geometry*

For the more general case of pendular rings $\bar{k} \neq 0$, the stability limits for the pin–pin disturbance are unaffected by the support geometry. No such statement can be made for the pin–free or free–free disturbances. However, relative stability for these disturbances can be inferred from the planar $\bar{k} = 0$ case. That is, for a fixed interface shape k, α, the shape on a concave solid support $(\bar{k} < 0)$ is relatively stable to that on a planar support $(\bar{k} = 0)$, which is relatively stable to that on a convex support $(\bar{k} > 0)$ (cf. Fig. 6).

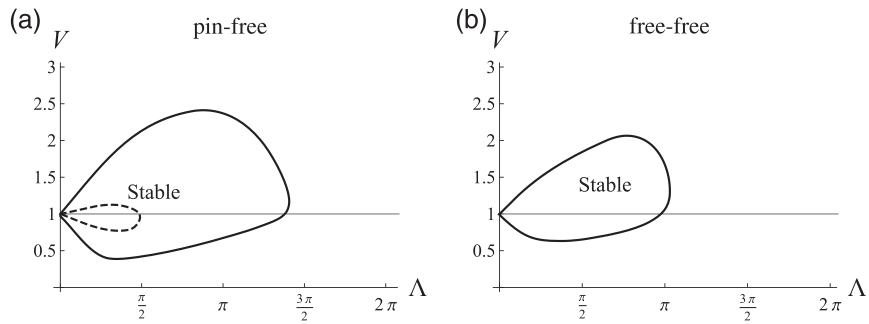

FIG. 5. Symmetric liquid bridge stability diagram for $\ell = 0$ in the length–volume (Λ, V) space for pin–free (a) and free–free (b) boundary conditions illustrating the stability boundaries for pressure (dashed) and volume (solid) disturbances. No bound was found to guarantee stability to pressure disturbances.

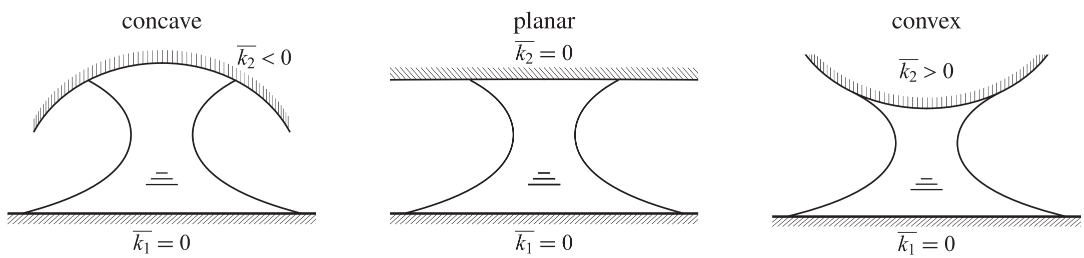

FIG. 6. Schematic of a liquid bridge with axisymmetric support geometry. For pin–free and free–free disturbances, the concave support $\bar{k}_2 < 0$ (left) is relatively stable to the planar support $\bar{k}_2 = 0$ (centre), which is relatively stable to the convex support $\bar{k}_2 > 0$ (right). For pin–pin disturbances, the stability limits are identical.

This result, which is summarized in Bostwick & Steen (2015, Section 3.2.2), follows directly from several theorems in Courant & Hilbert (1953) related to spectral monotonicity of self-adjoint operator equations with free disturbances.

The liquid bridge stability diagrams shown in Fig. 5 for $\bar{k}_1 = \bar{k}_2 = 0$ can be viewed as a slice of a larger parameter space that includes the support curvatures $\bar{k}_1, \bar{k}_2$. Relative stability for pin–free disturbances follows directly from the 1D homotopy for $\bar{k}_2$; the stability windows widen (shrink) for solid supports concave $\bar{k}_2 < 0$ (convex $\bar{k}_2 > 0$) to the interface. That is, base states that are stable for planar supports are also stable for concave supports. For free–free disturbances, relative stability is more complex as the homotopy from the planar state is 2D $\bar{k}_1 \neq \bar{k}_2 \neq 0$. When both supports are concave, these base states are relatively stable to the planar supports. However, in situations where one support is concave and the other convex, no immediate statement can be made with regard to relative stability.

4. Concluding remarks

We have developed the energy bounding method to find the static stability of the liquid bridge to disturbances with either (i) pinned or (ii) mobile contact lines. The goal is to provide quick stability checks on equilibrium solutions. In our method, the second variation of surface energy is manipulated into a quadratic form, which we bound from below to yield a critical functional. Finally, we utilize elementary results from the calculus of variations to generate our stability criteria. We illustrate the utility of our method by comparing our stability criteria to the Plateau limit for the liquid cylinder (Plateau, 1863) and the symmetric catenoid with pinned contact lines (Erle *et al.*, 1970). Our method is sharp for these classic problems. We also report new stability results for the catenoid and most-general symmetric liquid bridge between parallel plates with mobile contact-lines at one or both solid supports.

In general, stability calculations involve solving a complicated boundary value problem associated with the second variation or with computing conjugate points (Howe, 1887; Gillette & Dyson, 1971). Both of these methods prove to be cumbersome, because they involve direct calculations of the second variation. Alternative methods, such as the Poincaré–Maddocks theorems, employ tools of bifurcation theory that allows one to determine stability from families of equilibria, thereby bypassing direct calculation of the second variation (Maddocks, 1987; Lowry & Steen, 1995). The primary deficiency in the Poincaré–Maddocks method is that one must use continuation from a solution whose stability is known *a priori*. The strength of our method is that one does not need to construct a solution to the boundary value problem associated with the second variation. Only information regarding the equilibrium surface is required to generate the stability criteria for the pin–pin boundary conditions (2.24, 2.25). For the pin–free and free–free disturbances, we replace a complicated boundary value problem by a much simpler one which has a standard solution. Although our bounding method is clearly approximate, it can produce sharp bounds and requires very little computational effort, unlike most stability calculations.

Finally, we reiterate that our method generates sufficient conditions for stability. That is, if the bounding method criterion is satisfied, then the liquid bridge is stable. However, liquid bridges may be stable even though the criterion is not satisfied. This is seen in Fig. 4, where the stability envelopes for the bounding method are contained within the true stability envelopes; for slender $V < 1$ bridges the curves are nearly indistinguishable, illustrating the utility of our method. We also note that our method yields no predictions regarding when a liquid bridge may go unstable.

Funding

This work was supported by NASA Grant NNX09AI83G and NSF Grant CBET-1236582.

References

Bauer, H. (1992) Natural damped frequencies and axial response of a rotating finite viscous liquid column. *Acta Mech.*, **93**, 29–52.

Blaschke, W. (1930) *Vorlesungen über Differentialgeometrie I. Elementare Differentialgeometrie, Dritte Erweiterte Auflage*. Berlin: Springer.

Bolsa, O. (1904) *Lectures on the Calculus of Variations*. Chicago: University of Chicago Press.

Bostwick, J. & Steen, P. (2010) Stability of constrained cylindrical interfaces and the torus lift of Plateau-Rayleigh. *J. Fluid Mech.*, **647**, 201–219.

Bostwick, J. & Steen, P. (2013) Coupled oscillations of deformable spherical-cap droplets. Part 2. Viscous motions. *J. Fluid Mech.*, **714**, 336–360.

Bostwick, J. & Steen, P. (2015) Stability of constrained capillary surfaces. *Ann. Rev. Fluid Mech.*, **47**, 539–568.

Carter, W. (1988) The forces and behavior of fluids constrained by solids. *Acta Metall.*, **36**, 2283–2292.

Courant, R. & Hilbert, D. (1953) *Methods of Mathematical Physics*, vol. I. New York, NY: Wiley-Interscience Publications.

Davis, S. (1980) Moving contact lines and rivulet instabilities. Part 1. The static rivulet. *J. Fluid Mech.*, **98**, 225–242.

Delaunay, C. (1841) Sur la surface de révolution dont la courbure moyenne est constante. *J. Math Pure et App.*, **16**, 309–321.

Dodds, S., Carvalho, M. S. & Kumar, S. (2012) The dynamics of three-dimensional liquid bridges with pinned and moving contact lines. *J. Fluid Mech.*, **707**, 521–540.

Dupré, A. (1869) *Théorie Méchanique de La Chaleur*. Paris, France: Gauthier-Villars.

Elele, E., Shen, Y. & Khusid, B. (2010) Electrodeless electrohydrodynamic printing of personalized medicines. *Appl. Phys. Lett.*, **97**, 233501.

Elfring, G. J. & Lauga, E. (2012) Buckling instability of squeezed droplets. *Phys. Fluids*, **24**, 072102.

Erle, M., Gillette, R. & Dyson, D. (1970) Stability of interfaces of revolution with constant surface tension-the case of the catenoid. *Chem. Eng. J.*, **1**, 97–109.

Gillette, R. & Dyson, D. (1971) Stability of fluid interfaces of revolution between equal solid circular plates. *Chem. Eng. J.*, **2**, 44–54.

Gillette, R. & Dyson, D. (1972) Stability of axisymmetric liquid–fluid interfaces towards general disturbances. *Chem. Eng. J.*, **3**, 196–199.

Gillette, R. & Dyson, D. (1974) Stability of static configurations with applications to the theory of capillarity. *Arch. Ration. Mech. Anal.*, **53**, 150–177.

Howe, W. (1887) Friedrich-Wilhelms Universität zu Berlin. *Ph.D. Thesis*, Berlin.

Johns, L. & Narayanan, R. (2002) *Interfacial Instability*. New York: Springer.

Joseph, D. (1976) *Stability of Fluid Motions*. New York: Springer.

Langbein, D. (1992) Stability of liquid bridges between parallel plates. *8th European Symposium on Materials and Fluid Sciences in Microgravity*, vol. 1, pp. 85–93.

Langbein, D. (2002) *Capillary Surfaces: Shape–Stability–Dynamics, in Particular Under Weightlessness*. Springer.

Laplace, R. (1806) *An Essay on the Cohesion of Fluids*. Paris: Coureier.

Lowry, B. & Steen, P. (1995) Capillary surfaces: stability from families of equilibria with application to the liquid bridge. *Proc. R. Soc. Lond.*, **449**, 411–439.

Maddocks, J. (1987) Stability and folds. *ARMA*, **99**, 301–328.

Maxwell, J. (1898) *Encylopedia Britannica*, 9th edn. Edinburgh: Adam and Charles Black.

Michael, D. (1981) Meniscus stability. *Ann. Rev. Fluid Mech.*, **13**, 189–215.

Michael, D. & Williams, P. (1997) The equilibrium and stability of sessile drops. *Proc. Roy. Soc. Lond. A*, **354**, 127–136.

Myshkis, A., Babskii, V., Slobozhanin, N. & Tyuptsov, A. (1987) *Low-Gravity Fluid Mechanics*. Oxford: Springer.

Olbricht, W. L. (1996) Pore-scale prototypes of multiphase flow in porous media. *Annu. Rev. Fluid Mech.*, **28**, 187–213.

Orr, F. M., Scriven, L. E. & Rivas, A. P. (1975) Pendular rings between solids: meniscus properties and capillary force. *J. Fluid Mech.*, **67**, 723–742.

Padday, J. & Pitt, A. (1973) The stability of axisymmetric mensici. *Proc. R. Soc. A*, **275**, 489–528.

Plateau, J. (1863) Experimental and theoretical researches on the figures on equilibrium of a liquid mass withdrawn from the action of gravity. *A. Rep. Board Reg. Smithson. Inst.*, pp. 207–285.

Poincaré, H. (1885) Sur l'équilibre d'une masse fluide animée d'un mouvement de rotation. *Acta. Math.*, **7**, 259–380.

Quéré, D. (1999) Fluid coating on a fiber. *Annu. Rev. Fluid Mech.*, **31**, 347–384.

Rayleigh, L. (1879) On the capillary phenomenon of jets. *Proc. R. Soc. Lond.*, **29**, 71–97.

Russo, M. & Steen, P. (1986) Instability of rotund capillary bridges to general disturbances: experiment and theory. *J. Colloid Interface Sci.*, **113**, 154–163.

Slobozhanin, L., Alexander, J. I. D. & Resnick, A. (1997) Bifurcation of the equilibrium states of a weightless liquid bridge. *Phys. Fluids*, **9**, 1893–1905.

Steiner, J. (1882) *Gesammelte Werke*. Berlin, Germany: Reimer.

Stewart, J. (1995) *Calculus*. Pacific Grove, CA: Brooks/Cole Publishing.

Vogel, T. I. (1987) Stability of a liquid drop trapped between two parallel planes. *SIAM J. Appl. Math.*, **47**, 516–525.

Vogel, T. (1989) Stability of a liquid drop trapped between two parallel planes. II. General contact angles. *SIAM J. Appl. Math.*, **49**, 1009–1028.

Vogel, M. & Steen, P. (2010) Capillarity-based switchable adhesion. *Proc. Natl. Acad. Sci.*, **107**, 3377–3381.

Young, T. (1805) An essay on the cohesion of fluids. *Phil. Trans. R. Soc. Lond.*, **95**, 65–87.

Young, L. (2000) *Lectures on the Calculus of Variations and Optimal Control Theory*. Providence, RI: AMS Chelsea Publishing.